3D space-dependent models for stochastic dosimetry applied to exposure to low frequency magnetic fields

E Chiaramello, Laurent Le Brusquet, M. Parazzini, S. Fiocchi, M Bonato, P Ravazzani

3D space-dependent models for stochastic dosimetry applied to exposure to low frequency magnetic fields

E. Chiaramello[1], L. Le Brusquet[2], M. Parazzini[1], S. Fiocchi[1], M. Bonato[1], and P. Ravazzani[1]
[1]*Istituto di Elettronica e di Ingegneria dell'Informazione e delle Telecomunicazioni IEIIT CNR, Milano, Italy*
[2]*Département Signal et Statistiques Centrale Supélec Paris France*

Abstract

In this study, an innovative approach that combines Principal Component Analysis (PCA) and Gaussian process regression (Kriging method), never used before in the assessment of human exposure to electromagnetic fields, was applied to build space-dependent surrogate models of the 3D spatial distribution of the electric field induced in central nervous system of children of different age exposed to uniform magnetic field at 50 Hz with uncertain orientation. The 3D surrogate models showed very low normalized percentage mean square error values, confirming the feasibility and the accuracy of the approach in estimating the 3D spatial distribution of E with a low number of components. The electric field induced in children tissues were within the ICNIRP basic restrictions for general public and that no significant difference was found in the level of the exposure and in the 3D spatial distribution of the electric fields induced in tissues of children of different ages.

Introduction

The ubiquity of Extremely Low-Frequency Magnetic Fields (ELF-MF), such as those generated by transmission of electricity power lines, contributes to the raising of public awareness over the potential adverse health effects due to the interaction of ELF-MF with the human body. The exposure to ELF-MF of high amplitude causes well known acute biological effects on the nervous system, such as nerve stimulation and induction of retinal phosphenes [1]. Starting from the late 1970s, many studies focused on a possible association, firstly suggested by [2], between long-term exposure to ELF-EMF and an increased risk of childhood cancer (see e.g. [3]), leading the International Agency for Research on Cancer (IARC) [4] to classify ELF-MF as "possibly carcinogenic to humans" (2002).

Many studies investigated the exposure to magnetic field at the specific frequency of 50 Hz, particularly focusing on children [5], [6], and fetuses [5], [7]–[9], for their precocity of exposure. Most of these studies investigated the assessment of the compliance to exposure guidelines when considering few specific exposure scenarios, providing no information about how the exposure changes in realistic and

highly variable scenarios. Such an assessment is indeed a challenging task, due to the intrinsic variability of the parameters that influence the exposure, (e.g. morphology, anatomy and posture of the exposed subject, reciprocal position of the source and the exposed subject, polarization of the EMF field [10]). Classical electromagnetic computational techniques typically involve highly time-consuming simulations to obtain 3D spatial distributions of the electromagnetic fields induced in human tissues, making almost impossible to characterize how the exposure changes in variable conditions. Recently, stochastic dosimetry has been proposed as a method to face variability of the EMF exposure scenario in the assessment of exposure. Stochastic dosimetry uses statistics to build surrogate models able to replace by analytical equations the heavy numerical simulations that would be needed to describe the highly variable exposure by electromagnetic computational techniques. Stochastic dosimetry proved to be a useful method to assess the EMF exposure both at radio frequency [11]–[13] and at low frequency [14], [15]. All these studies were exclusively dealing with surrogate models of EMF univariate variables, e.g. the 99^{th} percentile calculated on the 3D domain of root mean square tissue-specific values of the electric field (E) induced by ELF-MF [14]. However, a complete assessment should involve the complete description of the 3D spatial distribution of the induced E in each tissue of the exposed subjects in variable conditions, as different spatial localization of the peak, for example, could involve different effect on the tissues. Such an assessment involves creating surrogate models able to describe the 3D spatial distribution of E induced in each tissue. Possible approaches to face the problem of creating surrogate models of output variables dependent on time-space coordinates could be to treat these coordinates as additional input variables [16], [17] or to build a separate surrogate model for each coordinate dependent observation. Both these approaches involve a big computational effort, restricting the analysis to low dimensional problems. Some recent studies focused on the developing of non-intrusive methods (i.e. methods in which the phenomenon to be approximated is treated as a "black-box") for building surrogate models of space-temporal variables [18]–[20]. The main novelty of these approaches is to reduce the high dimensional output to a low-dimensional vector hypothesizing that variables at nearby temporal and spatial coordinates are highly correlated [21] and then to develop surrogate models for predicting each component of the vector.

In this study an innovative approach that combines Principal Component Analysis (PCA) and Gaussian process regression (Kriging method) [18] to build space-dependent surrogate models was used to assess the variability of 3D spatial distribution of EMF induced in human tissues in variable and uncertain exposure conditions. This method, never applied before for the assessment of human exposure to electromagnetic fields, was validated and used to evaluate the variability of the 3D spatial distribution of

E induced in children tissues when exposed to a uniform 50 Hz magnetic field with uncertain orientation. The starting point of this assessment was a previous study [14], in which a stochastic approach based on polynomial chaos expansions was used to assess the variability of the 99th percentile of the E induced by magnetic field with variable orientation. The main novelty of the present study was the possibility of assessing not only the variability of E as a univariate and summarizing variable, such as the 99th percentile, but considering its complete 3D spatial distribution for each possible orientation of the magnetic field, thus obtaining a complete description of E without the need of time consuming computational simulations.

Materials and Methods

The E induced in the head nervous tissues of three children of five, eight and fourteen years was assessed by varying the orientation of a perfectly homogeneous 50 Hz B-field of 200 μT of amplitude, using 3D surrogate models. Each surrogate model describes how the 3D variable of interest Y (i.e., the E induced in the brain) was affected by the variability in the input parameters X (i.e., the different orientation of the **B**-field). Three main steps composed the experimental procedure. The first step, namely, "design of the experiment," consisted of using deterministic dosimetry, that is, dosimetry based on computational methods, for the evaluation of a set of N experimental observations Y_0 of the variable of interest Y, needed for the construction of the surrogate models. The second step, namely, "3D surrogate modelling," focused on the development and validation of a surrogate model $\hat{Y}$. The surrogate models thus obtained were used to obtain a complete description of the 3D E distributions for all the possible orientations of the magnetic field (in the "analysis of the 3D exposure" step). Details about each step are as follows.

A. Design of the experiment

The set of N experimental observations Y_0 of the variable of interest Y, needed for the construction of the 3D surrogate models, was obtained by the same procedure and simulations used in [14]. The random input vector X was defined as the two spherical angles theta (θ) and phi (φ), which characterized the $\boldsymbol{B}$-field orientation. The experimental design X_0 has been generated using a Latin Hypercube Sampling (LHS), using a selection criterion based on the maximum of the minimum distance between the points [22]. The variable of interest Y is a matrix containing the root mean square value of E averaged on a 2 mm side cube in each point of the tissues of the central nervous system (CNS) contained in the head, i.e. brain grey matter, brain white matter, cerebellum, commissure anterior, commissure posterior, hippocampus, hypothalamus, medulla oblongata, midbrain, pons, pinealbody and thalamus. The simulations were conducted by deterministic dosimetry based on Magneto Quasi-Static low frequency

solver implemented on the simulation platform SEMCAD X (Schmid & Partner Engineering), using three high resolution children models, namely Roberta, Eartha and Louis of five, eight and fourteen years from the Virtual Classroom [23]. The dielectric properties (permittivity and conductivity values) in each tissue of the children were assigned according to the data available in literature [24], [25]. A total number of $N = 150$ simulations, corresponding to 150 different orientations of B-field were carried out to obtain the set of observation Y_0. Each observation is a matrix of dimension 334x203x1102 for Roberta, 448x231x1385 for Eartha and 483x296x1726, containing the 2 mm-averaged root mean square E values in all the above mentioned tissues. The set Y_0 was divided into a training set $Y_{training}$, consisting of 100 observations and used to build the 3D surrogate models, and a validation set $Y_{validation}$ of 50 observations used to validate the obtained models.

B. 3D Surrogate modelling

Similarly to the approach proposed by [18], the 3D surrogate modelling procedure is based on three main steps. First, a kernel PCA with linear kernel was applied. The rationale of using PCA is that the E induced at nearby spatial coordinates could be hypothesized to be highly correlated [26], and thus can be efficiently represented by a few d components. The central idea of PCA is to project the original D dimensional data y into a space were the variance is maximized

$$y = Zw + \mu + e \qquad (1)$$

where Z refers to the matrix of eigenvectors of the data covariance matrix corresponding to the d ($d<D$) largest eigenvalues, w refers to the weights used to construct the new axis, μ is the mean value of the data and e is the residual error.

As a second step, the Kriging method (see, e.g. [18]) was applied to develop a separate surrogate model for each of the d components identified by PCA (i.e. for each of the d column of the matrix Z). Kriging (a.k.a. Gaussian process modelling) is a stochastic interpolation algorithm that assumes that a model output a realization of a Gaussian process indexed by $x \in D_X \subset \mathbb{R}^M$. A Kriging surrogate model is described by the following equation:

$$M^K(x, \omega) = \beta^T f(x) + \sigma^2 Z(x, \omega) \qquad (2)$$

where $\beta^T f(x)$, is the mean value of the Gaussian process and it consists of the regression coefficients $\{\beta_j , j = 1, \ldots , P\}$ and the basis functions $\{f_j , j = 1, \ldots , P\}$, σ^2 is the variance of the Gaussian process, $Z(x, \omega)$ is a zero mean, unit variance, stationary Gaussian process. The term ω describes outcomes of the underlying probability space with a correlation function R (a.k.a. correlation family) and its hyperparameters θ. The correlation function $R = R(x, x', \theta)$ models the dependence structure between values at different points, e.g. x and x', and depends on the hyperparameters θ. In this study, a Matérn

correlation function R was used and its hyperparameters σ^2 and θ were estimated by Maximum Likelihood Estimation (MLE).

The third step in the 3D surrogate modelling procedure consisted of using the inverse Principal Component analysis to reconstruct, from the univariate surrogate models $\hat{f}_1$, $\hat{f}_2$, …, $\hat{f}_d$ obtained by Kriging method, the 3D spatial distribution of the E induced in the brain of the child. For more details about each step and about the whole 3D surrogate modelling procedure, see [18].

The 3D surrogate model $\hat{Y}$ built using the subset $Y_{training}$ was then validated on the subset $Y_{validation}$. The normalized Mean Square Error (MSE) between the values estimated by the 3D surrogate model $\hat{Y}$ and those obtained by deterministic dosimetry was computed as:

$$MSE = 100 * \sum_{i=1}^{N} \frac{\|\hat{Y}(\theta_i,\varphi_i) - Y_{validation}\|^2}{\|Y_{validation} - mean(Y_{validation})\|^2} \qquad (3)$$

C. Analysis of the 3D exposure

Once a 3D surrogate model has been built for the tissues of Roberta, Eartha and Louis, several orientations of the B-field have been randomly selected. As the computational effort in assessing the exposure using the 3D surrogate models was low, a high number (i.e., 1000) of orientations of the **B**-field was considered, in order to cover the range of variations of the input parameters. The E values induced in all the points of the children tissues by each specific $\boldsymbol{B}$-field orientation have then been calculated by means of the 3D surrogate models.

A statistical analysis has been performed to assess the variability of the exposure due to the change of orientation of the $\boldsymbol{B}$-field, in terms of Quartile Coefficient of Dispersion (QCD), calculated in each point of the considered tissues as:

$$QCD = \frac{Q_3 - Q_1}{Q_3 + Q_1} \qquad (4)$$

where Q_1 and Q_3 are, respectively, the first and the third percentiles of the distribution of E values obtained for the several orientation.

Results

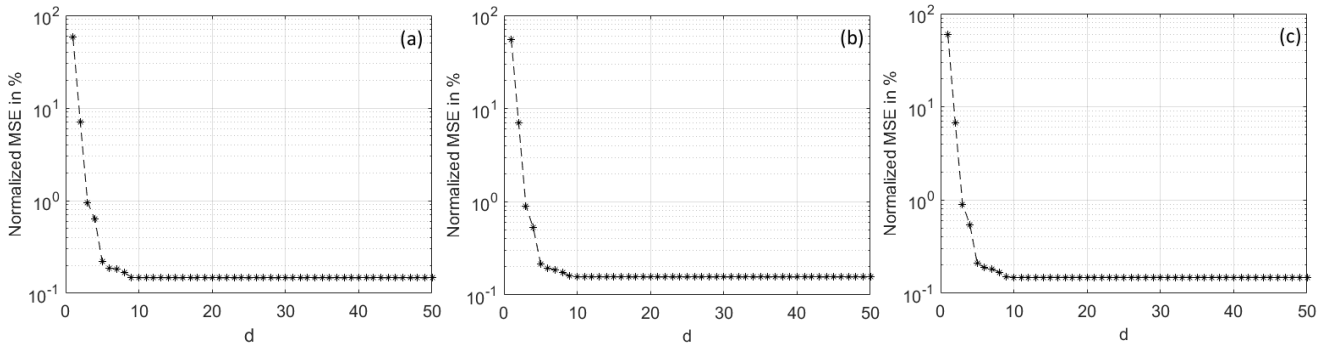

Figure 1: Normalized MSE versus the number *d* of components considered in the 3D surrogate modelling procedure, for Roberta (a), Eartha (b) and Louis (c) models.

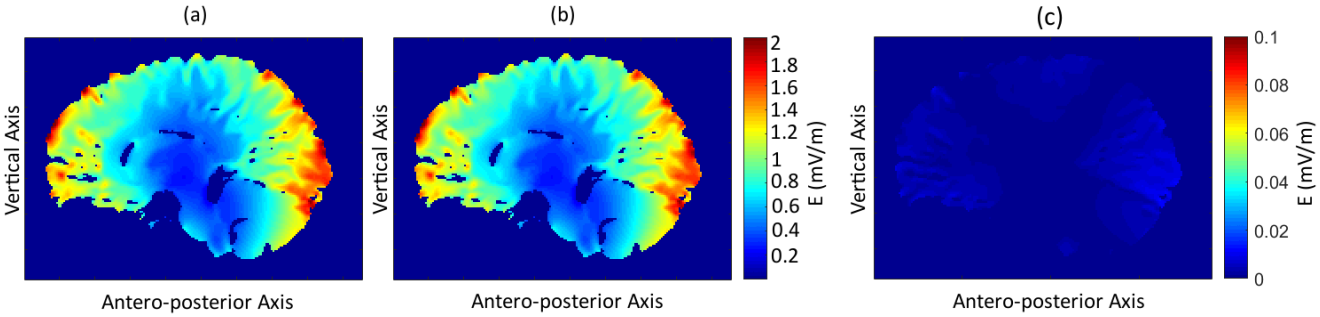

Figure 2: Spatial distribution of the electric field induced on one slice of Roberta's CNS tissues obtained by 3D surrogate model (a) and deterministic dosimetry (b).

Fig. 1 shows the MSE calculated on the validation set versus the number *d* of principal components considered in the 3D surrogate modelling procedure, for Roberta (fig.1a), Eartha (fig. 1b) and Louis (fig. 1c). For *d* equal to 10, the MSE was equal to 0.16%, 0.15% and 0.15%, for Roberta, Eartha and Louis, respectively, thus indicating that a low number of components was sufficient to represent the 3D distribution of E induced in children tissues with a very low validation error. The number *d* of components used to build the 3D surrogate models was therefore set equal to 10. As an example of reconstructed signal, fig. 2 shows the spatial distribution of the E induced on one slice of Roberta's CNS tissues obtained for one specific orientation (θ and φ equal to 35° and -150°, respectively) of the incident **B**-field by the 3D surrogate model (fig. 2a) and by deterministic dosimetry (fig. 2b) and their point to point difference (fig. 2c). Fig.2a and fig. 2b appear to be almost identical, and their differences are very small, lower than 0.035 mV/m (fig. 2c), confirming the feasibility of the proposed approach.

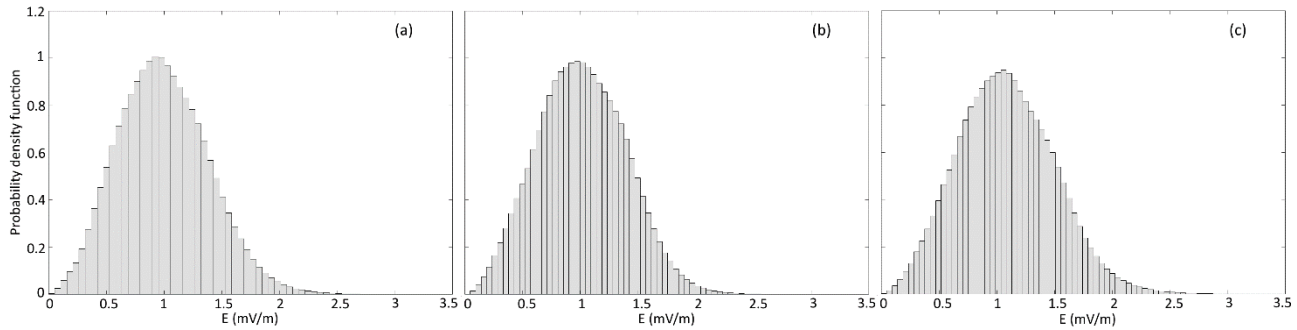

Figure 3: Normalized histograms of the E values obtained for 1000 orientations of the **B**-field in Roberta's CNS tissues (a), Eartha's tissues (b) and Louis's tissues (c).

Fig. 3 shows the normalized histograms of the *E* values for each points of the children CNS tissues obtained by the surrogate models for 1000 possible orientations of the **B**-field. The histograms obtained for Roberta (fig. 3a), Eartha (fig. 3b), and Louis (fig. 3c) were quite similar. For Roberta we found mean, median and max *E* values equal to 1 mV/m, 0.78 mV/m, and 3.12 mV/m, respectively. For Eartha we found mean, median and max *E* values equal to 1.02 mV/m, 1 mV/m, and 3.5 mV/m, respectively. For Louis we found mean, median and max *E* values equal to 1.1 mV/m, 1.06 mV/m, and 3.7 mV/m, respectively. For all the considered children, *E* values higher or equal to 90% of the maximum value obtained for each **B**-field orientation were localized in the brain grey matter. For each **B**-field orientation the 99th percentiles of the 3D distribution of the root mean square *E* values have been calculated. The values of E_{99th} were found to be almost equal across the three children, with median values in the range 1.9–2.1 mV/m and maximum values in the range 2.2–2.4 mV/m.

Fig. 4 shows, for each point of the frontal slice (a, d, g), horizontal slice (b, e, h) and sagittal slice (c, f, i) of CNS tissues passing through to the middle points on the head, the maximum values of the E induced by 1000 different ***B***-field orientations. Despite the small anatomical differences between the children of different age, the spatial distribution of the values of *E* were found to be quite similar: the highest maximum values, in the range 1.5-2.5 mV/m were placed on the more superficial portion of the tissues, in particular of the brain gray matter, while values in the range 1-1.5 mV/m were found on the more internal tissues, in particular in the brain gray and brain white matter. In the deeper CNS tissues, the maximum *E* values among those induced by the 1000 **B**-field orientations were found to be lower than 1 mV/m.

Fig. 5 shows, for the same tissue slices previously shown in fig. 4, the QCD values calculated in each point of children CNS tissues for 1000 orientations of the B-field. The variability of the exposure was

quite low, resulting in QCD values in the range 10^{-5}-0.13 with mean value equal to 0.01 for Roberta, QCD values in the range 10^{-5}-0.18 with mean value equal to 0.01 for Eartha, and QCD values in the range 10^{-5}-0.18 with mean value equal to 0.01 for Louis. For all the children, the frontal slices (fig. 5a, 5d and 5g) show the highest QCD values along the vertical and medio-lateral axes, especially for the more superficial positions. The horizontal (fig. 5b, 5e and 5h) and sagittal slices (fig. 5c, 5f and 5i) show a similar but less accentuated behavior, with QCD values higher than the mean value along almost all the external surface of the considered portion of CNS tissue.

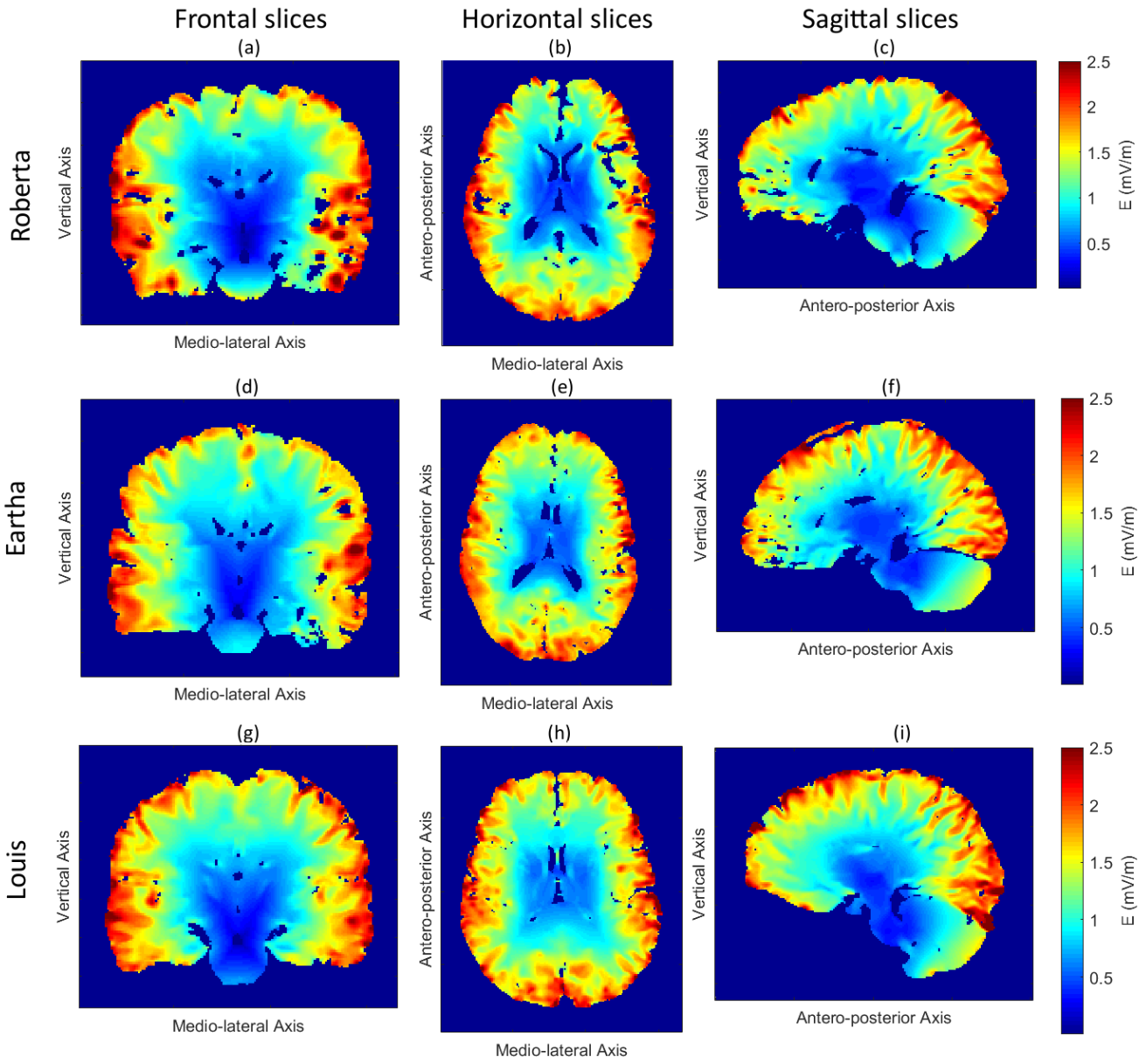

Figure 4: Maximum value induced in children tissues for 1000 orientations of the **B**-field: frontal (a,d,g), horizontal (b,e,h) and sagittal (c,f,i) slices, for Roberta (first row), Eartha (second row) and Louis (third row).

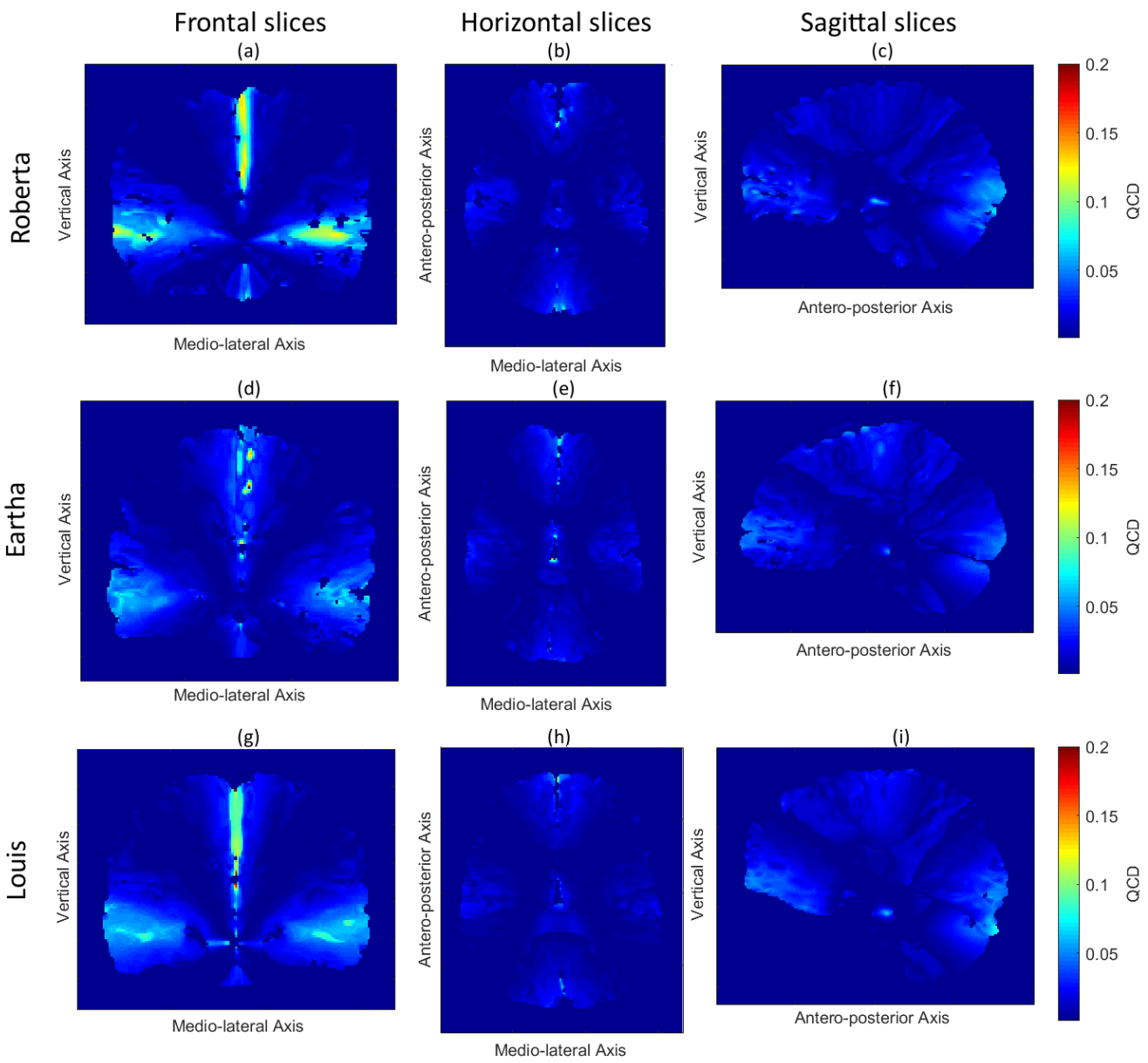

Figure 5: QCD values calculated for 1000 orientations of the **B**-field in each point of the frontal (a,d,g), horizontal (b,e,h) and sagittal (c,f,i) slices, for Roberta (first row), Eartha (second row) and Louis (third row).

Discussion and conclusions

In this study an innovative approach that combines Principal Component Analysis (PCA) and Gaussian process regression (Kriging method) was used for the first time in the electromagnetic dosimetry framework in order to assess the variability of the 3D spatial distribution of E in human tissues when exposed to EMF in variable and uncertain conditions. This method represents a step ahead compared to the approaches commonly used in stochastic dosimetry (see, e.g. [11], [12]), typically focused on the use of surrogate models to describe the variability of the exposure in uncertain conditions by summarizing

the exposure description by univariate and summarizing parameters, as allowed considering the full 3D spatial description of the EMF induced in tissues with small computational effort. Extending a previous study [14], the method was applied to assess the variability of 3D spatial distribution of E in children CNS exposed to a homogeneous magnetic field at 50 Hz of 200 μT of amplitude with uncertain orientation.

Even if the matrix to be modelled had big dimensions, up to 483x296x1726 points for Louis, only ten principal components were needed to reach very low normalized percentage MSE by the 3D surrogate modelling procedure. This finding, well expected, means that room mean square *E* values at nearby spatial coordinates were highly correlated, confirming the feasibility of using a PCA approach for reducing the complexity of the output. Moreover, the low normalized percentage MSE values obtained on the validation set confirmed the feasibility and the accuracy of the approach in estimating the 3D spatial distribution of E induced in children tissues for orientations of the ***B***-field not used to build the surrogate model. It should be noted that only one 3D surrogate model was needed to evaluate the *E* values in each point of all the tissues. In order to extract information about E induced in a specific tissue, it is sufficient to analyze the corresponding spatial coordinates. Once obtained the full description of the *E* values in each point of the considered tissues, it is possible to extract a-posteriori different information, e.g. the 99th percentile of the *E* values, coherently with the International Commission of Non-Ionizing Radiation Protection (ICNIRP) guidelines [28].

The 3D surrogate models were used to investigate the exposure in three high resolution anatomical models of children aging from five to fourteen years, evaluating the E induced in each point of the CNS contained in the head for 1000 different orientations of the magnetic field.

Maximum values of *E* were almost equal across the three children, in the range 3.12–3.7 mV/m, while the 99th percentiles of the *E* values obtained for each orientation were found to have median values in the range 1.9–2.1 mV/m and maximum values in the range 2.2–2.4 mV/m. These values were significantly below the International Commission of Non-Ionizing Radiation Protection (ICNIRP) basic restrictions for the general public exposure [28], coherently with findings by previous studies [6], [14].

The spatial distribution of the values of *E* were found to be quite similar for the three children: the highest values were localized on the more external tissues, in particular in the grey and white brain matter, while, as for the remaining tissues, the less superficial the tissue, the lower the induced *E* values. This finding

is coherent with results by previous studies [6], [14] in which the highest values of E_{99th} were observed in the brain grey matter tissue.

The variability of the exposure in each point of the considered tissues when varying the orientation of the magnetic fields resulted in QCD values always lower than 20%, similarly to previous findings by other studies [6], [14]. The variation of the orientation of the magnetic field influenced the exposure differently in different areas of the considered tissues, with the highest QCD values along the antero-posterior, vertical and medio-lateral axes and in those points near to the external surface.

In previous studies authors did not find consistent pattern as a function of age in the exposure to ELF-MF of children of different age [5], [6], [14]. Findings of this study confirmed that no significant difference was highlighted not only in the level of exposure of children of different ages when considering a high number of orientations of the magnetic field, but also in the spatial distribution of the induced *E* values.

In conclusion, the proposed approach that combines Principal Component Analysis (PCA) and Gaussian process regression (Kriging method) in order to build space-dependent surrogate models was found to be feasible to assess the 3D spatial distribution of E induced in human tissues when exposed to a uniform magnetic field with variable orientation. The proposed method allowed not only to assess the exposure to ELF-MF in terms of univariate parameters resuming the level of exposure, but to investigate how the 3D spatial distribution of EMF in human tissue is influenced by the variability intrinsic to realistic exposure scenarios. The possibility of considering such a level of complexity without huge computational efforts offers new tools to deal with the uncertainty, heterogeneity and complexity of the incoming 5G exposure scenarios, representing an important step towards a fully stochastic characterization of the exposure to EMF.

ACKNOWLEDGEMENT

This research is supported by the French National Research Program for Environmental and Occupational Health of ANSES (2015/1/202): Project ELFSTAT - In depth evaluation of children's exposure to ELF (40 – 800 Hz) magnetic fields and implications for health risk of new technologies, 2015-2019. The authors wish to thank Schmid and Partner Engineering AG (www.speag.com) for having provided the simulation software SEMCAD X/SIM4Life.

References

[1] R. D. Saunders and J. G. R. Jefferys, “A neurobiological basis for ELF guidelines.,” *Health Phys.*, vol. 92, no. 6, pp. 596–603, 2007.

[2] N. Wertheimer and E. Leeper, “Electrical wiring configurations and childhood cancer.,” *Am. J. Epidemiol.*, vol. 109, no. 3, pp. 273–284, 1979.

[3] L. Kheifets, A. Ahlbom, C. M. Crespi, G. Draper, J. Hagihara, R. M. Lowenthal, G. Mezei, S. Oksuzyan, J. Schüz, J. Swanson, A. Tittarelli, M. Vinceti, and V. Wunsch Filho, “Pooled analysis of recent studies on magnetic fields and childhood leukaemia.,” *Br. J. Cancer*, vol. 103, no. 7, pp. 1128–1135, 2010.

[4] Iarc, “International Agency for Research on Cancer Iarc Monographs on the Evaluation of Carcinogenic Risks To Humans,” *Iarc Monogr. Eval. Carcinog. Risks To Humans*, vol. 96, p. i-ix+1-390, 2002.

[5] P. Dimbylow and R. Findlay, “The effects of body posture, anatomy, age and pregnancy on the calculation of induced current densities at 50 Hz.,” *Radiat. Prot. Dosimetry*, vol. 139, no. 4, pp. 532–538, 2010.

[6] J. F. Bakker, M. M. Paulides, E. Neufeld, a Christ, X. L. Chen, N. Kuster, and G. C. van Rhoon, “Children and adults exposed to low-frequency magnetic fields at the ICNIRP reference levels: theoretical assessment of the induced electric fields,” *Phys. Med. Biol.*, vol. 57, no. 7, pp. 1815–1829, 2012.

[7] R. Cech, N. Leitgeb, and M. Pediaditis, “Fetal exposure to low frequency electric and magnetic fields.,” *Phys. Med. Biol.*, vol. 52, no. 4, pp. 879–888, 2007.

[8] A. Zupanic, B. . Valic, and D. Miklavcic, “Numerical assessment of induced current densities for pregnant women exposed to 50 Hz electromagnetic field,” *Int. Feder. Med. Biol. Eng. Proc*, vol. 16, pp. 226–229, 2007.

[9] I. Liorni, M. Parazzini, S. Fiocchi, M. Douglas, M. Capstick, M.-C. Gosselin, N. Kuster, and P. Ravazzani, “Dosimetric study of fetal exposure to uniform magnetic fields at 50 Hz,” *Bioelectromagnetics*, vol. 597, no. 35(8), pp. 580–97, 2014.

[10] J. Wiart, *Radio-Frequency Human Exposure Assessment: From Deterministic to Stochastic Methods*. John Wiley & Sons, ISTE, 2016.

[11] E. Chiaramello, M. Parazzini, S. Fiocchi, P. Ravazzani, and J. Wiart, “Assessment of Fetal Exposure to 4G LTE Tablet in Realistic Scenarios : Effect of Position , Gestational Age and Frequency,” *IEEE J. Electromagn. RF Microwaves Med. Biol.*, vol. 1, pp. 26–33, 2017.

[12] E. Chiaramello, M. Parazzini, S. Fiocchi, P. Ravazzani, and J. Wiart, “Stochastic Dosimetry based on Low Rank Tensor Approximations for the Assessment of Children Exposure to WLAN Source,” *IEEE J. Electromagn. RF Microwaves Med. Biol.*, 2018.

[13] E. Chiaramello, M. Parazzini, S. Fiocchi, M. Bonato, P. Ravazzani, and J. Wiart, “Stochastic Exposure Assessment to 4G LTE femtocell in indoor environments,” in *2nd URSI Atlantic Radio Science Meeting*.

[14] E. Chiaramello, S. Fiocchi, P. Ravazzani, and M. Parazzini, “Stochastic Dosimetry for the Assessment of Children Exposure to Uniform 50 Hz Magnetic Field with Uncertain Orientation,” *Biomed Res. Int.*, vol. 2017, pp. 1–14, 2017.

[15] S. Fiocchi, E. Chiaramello, M. Parazzini, and P. Ravazzani, “Influence of tissue conductivity on foetal exposure to extremely low frequency magnetic fields at 50 Hz using stochastic dosimetry,” *PLoS One*, vol. 13, no. 2, 2018.

[16] M. C. Kennedy and A. O’Hagan, “Bayesian calibration of computer models,” *J. R. Stat. Soc. Ser. B (Statistical Methodol.)*, vol. 63, no. 3, pp. 425–464, 2001.

[17] J. Zhang, A. J. Morris, E. B. Martin, and C. Kiparissides, “Prediction of polymer quality in batch polymerisation reactors using robust neural networks,” *Chem. Eng. J.*, vol. 69, no. 2, pp. 135–143, 1998.

[18] T. Chen, K. Hadinoto, W. Yan, and Y. Ma, “Efficient meta-modelling of complex process simulations with time – space-dependent outputs,” *Comput. Chem. Eng.*, vol. 35, no. 3, pp. 502–509, 2011.

[19] O. T. Kajero, R. B. Thorpe, T. Chen, B. Wang, and L. Le, “Kriging Meta-Model Assisted Calibration of Computational Fluid Dynamics Models,” *AIChE J.*, vol. 62, no. 12, pp. 4308–4320, 2016.

[20] L. Hawchar, C. El Soueidy, and F. Schoefs, “Principal component analysis and polynomial chaos expansion for time-variant reliability problems,” *Reliab. Eng. Syst. Saf.*, vol. 167, pp. 406–416, 2017.

[21] D. Gay and H. Ray, “Identification and control of distributed parameter systems by means of the singular value decomposition,” *Chem. Eng. Sci.*, vol. 50, no. 10, pp. 1519–1539, 1995.

[22] G. Blatman, “Adaptive sparse polynomial chaos expansions foruncertainty propagation and sensitivity analysis,” Université Blaise Pascal, Clermont-Ferrand, 2009.

[23] M.-C. Gosselin, E. Neufeld, H. Moser, E. Huber, S. Farcito, L. Gerber, M. Jedensjö, I. Hilber, F. Di Gennaro, B. Lloyd, E. Cherubini, D. Szczerba, W. Kainz, and N. Kuster, “Development of a new generation of high-resolution anatomical models for medical device evaluation: the Virtual Population 3.0.,” *Phys. Med. Biol.*, vol. 59, no. 18, pp. 5287–5303, 2014.

[24] C. Gabriel, S. Gabriel, and E. Corthout, “The dielectric properties of biological tissues .1. Literature survey,” *Phys. Med. Biol.*, vol. 41, no. 11, pp. 2231–2249, 1996.

[25] C. Gabriel, a Peyman, and E. H. Grant, “Electrical conductivity of tissue at frequencies below 1 MHz.,” *Phys. Med. Biol.*, vol. 54, no. 16, pp. 4863–4878, 2009.

[26] J. Rougier, “Efficient emulators for multivariate deterministic functions,” *J. Comput. Graph. Stat.*, vol. 17, pp. 827–843, 2008.

[27] S. Fiocchi, I. Liorni, M. Parazzini, and P. Ravazzani, “Assessment of foetal exposure to the homogeneous magnetic field harmonic spectrum generated by electricity transmission and distribution networks,” *Int. J. Environ. Res. Public Health*, vol. 12, no. 4, pp. 3667–3690, 2015.

[28] ICNIRP-International Commission of Non-Ionizing Radiation Protection., “Guidlines for limiting exposure to time varying electric and magnetic fields (1 Hz to 100 kHz).,” *Heal. Phys*, vol. 99, pp. 818–836, 2010.